Inorganic Chemistry

· Article

Coexistence of Five Different Copper(II)–Phenanthroline Species in the Crystal Packing of Inorganic–Metalorganic Hybrids Based on Keggin Polyoxometalates and Copper(II)–Phenanthroline–Oxalate Complexes

Santiago Reinoso,[†] Pablo Vitoria, Juan M. Gutiérrez-Zorrilla,* Luis Lezama,* Juan M. Madariaga,[‡] Leire San Felices, and Amaia Iturrospe

Departamento de Química Inorgánica, Facultad de Ciencia y Tecnología, Universidad del País Vasco, P. O. Box 644, E-48080 Bilbao, Spain

Reaction of in situ generated copper(II)-monosubstituted Keggin polyoxometalates and copper(II)–phenanthroline–oxalato complexes in ammonium or rubidium acetate buffers led to the formation of the hybrid inorganic–metalorganic compounds E$_4$[Cu(phen)(H$_2$O)$_4$]$_2$[Cu$_4$(phen)$_4$(H$_2$O)$_4$(ox)$_3$]$_{0.6}$[Cu$_2$(phen)$_2$(H$_2$O)$_4$(ox)]$_{0.4}$[Cu(phen)(ox)]$_{0.8}$[{SiW$_{11}$O$_{39}$Cu-(H$_2$O)}$_2${Cu$_2$(phen)$_2$(ox)}]·20H$_2$O [E: Rb (**1**), NH$_4$ (**2**)]. The two compounds have been characterized by means of elemental analysis, thermogravimetry, infrared and electron paramagnetic resonance spectroscopies, and magnetic susceptibility measurements, and their structures have been established by single-crystal X-ray diffraction. Both compounds are isostructural, and they contain a discrete bimolecular hybrid polyanion and several types of copper–phenanthroline complexes of variable nuclearity. The main structural features of these compounds are the presence of the new hybrid POM [{SiW$_{11}$O$_{39}$Cu(H$_2$O)}$_2${Cu$_2$(phen)$_2$(μ-ox)}]$^{10-}$, where the dinuclear copper–oxalato complex is sandwiched by two copper-monosubstituted POMs, and the coexistence of five different copper–phenanthroline species with nuclearities ranging from one to four.

Introduction

Polyoxometalates (POMs)[1] are anionic metal−oxygen clusters that exhibit a remarkable molecular, electronic, and structural diversity. These features endow them with applications in a wide range of fields including catalysis,[2] magnetism, material science,[3] and medicinal chemistry.[4]

A recent trend in POM chemistry has been the functionalization of polyoxometalate anions to extend their versatility and lead to new and more selective applications. The chemistry of POM-based hybrids has been significantly enriched by the inclusion of transition metal (TM) coordination complexes into the hybrid system, either to provide charge compensation or as a part of the inorganic POM framework itself.[5] Given the importance of precise compositions and structures in all investigations focused on this class of clusters, the research toward understanding the self-assembly processes that support the formation of polyoxometalate hybrids has to be a route to enable the preparation of multifunctional materials, which take advantage of the unique physical properties associated with this class of compounds.[6]

Currently, we are interested in exploring the applicability of Keggin-POMs and TM-carboxylate cationic complexes in the preparation of new hybrid compounds.[7] The interest of supporting TM-carboxylate complexes, which have been extensively studied in magnetostructural research works, on Keggin POMs lies on the possibility of tuning the magnetic properties due to their high dependence on the nature and spatial disposition of the ligands.

* To whom correspondence should be addressed. E-mail: luis.lezama@ehu.es (L.L.), juanma.zorrilla@ehu.es (J.M.G.-Z.). Fax: +34946013500.
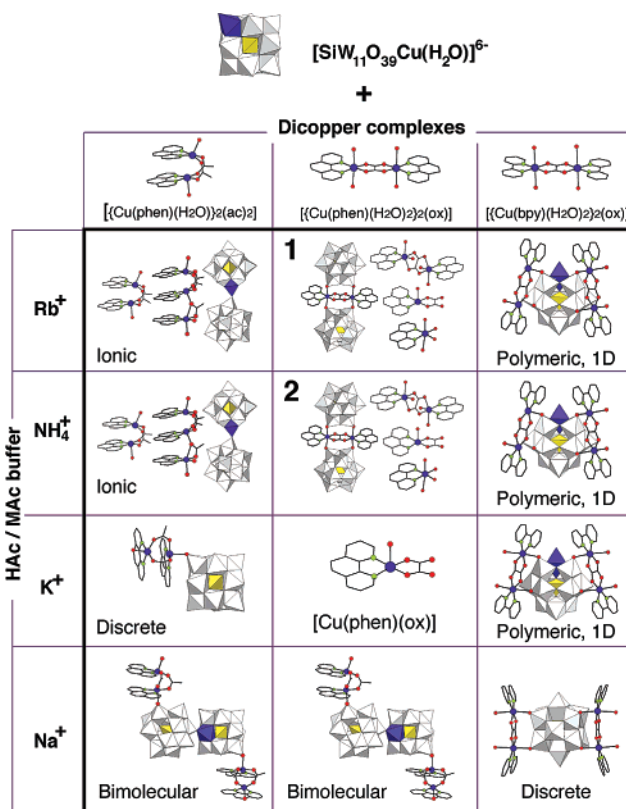
† Current address: Jacobs University Bremen, School of Engineering and Science, P. O. Box 750 561, 28725 Bremen, Germany.

‡ Departamento de Química Analítica, Facultad de Ciencia y Tecnología, Universidad del País Vasco, P. O. Box 644, E-48080 Bilbao, Spain.

(1) (a) Pope, M. T.; Müller, A. *Angew. Chem., Int. Ed. Engl.* **1991**, *30*, 34. (b) *Polyoxometalates: From Platonic Solids to Antiretroviral Activity*; Pope, M. T., Müller, A., Eds.; Kluwer: Dordrecht, The Netherlands, 1994. (c) Hill, C. L. Ed. *Chem. Rev.* **1998**, *98* (1), special thematic issue. (d) *Polyoxometalate Chemistry: From Topology via self-Assembly to Applications*; Pope, M. T., Müller, A., Eds.; Kluwer: Dordrecht, The Netherlands, 2001. (e) *Polyoxometalate Chemistry for Nanocomposite Design*; Pope, M. T., Yamase, T., Eds.; Kluwer: Dordrecht, The Netherlands, 2002. (f) *Polyoxometalate Molecular Science*; Borrás-Almenar, J. J., Coronado, E., Müller, A., Pope, M. T., Eds.; Kluwer: Dordrecht, The Netherlands, 2003. (g) Pope, M. T. In *Comprehensive Coordination Chemistry II*; McCleverty, J. A., Meyer, T. J., Eds.; Elsevier Ltd.: Oxford, U.K., 2004; Vol. 4, Chapter 10.

Copper(II)−Phenanthroline Species

With the aim of studying the influence of the reaction media over the final products, reactions of in situ generated $[SiW_{11}O_{39}Cu(H_2O)]^{6-}$ (starting from the potassium salt of $[SiW_{11}O_{39}]^{8-}$ as POM precursor) and several dinuclear copper(II)-bridging carboxylate cationic complexes ([{Cu-(phen)(H_2O)}_2(ac)_2]^{2+}, [{Cu(bpy)(H_2O)_2}_2(ox)]^{2+}, and [{Cu-(bpy)(H_2O)_2}_2(ox)]^{2+}, where phen = 1,10-phenanthroline, bpy = 2,2′-bipyridine, ac = acetate, and ox = oxalate) were carried out in four different acetic acid/alkaline acetate buffer solutions, HAc/MAc, where M = Na⁺, K⁺, Rb⁺, and NH₄⁺. As can be seen in Scheme 1, when the buffer solution is made of rubidium or ammonium acetate, these cations

(2) (a) Misono, M. *Catal. Rev.*−Sci. Eng. **1988**, *30,* 339. (b) Ilkenhaus, T.; Herzorg, B.; Braun, T.; Schlögl, R. *J. Catal.* **1995**, *153*, 275. (c) Belanger, R.; Moffat, J. B. *J. Catal.* **1995**, *152*, 171. (d) Corma, A. *Chem. Rev.* **1995**, *95*, 559. (e) Hill, C. L.; Prosser-Mccartha, M. *Coord. Chem. Rev.* **1995**, *143*, 407. (f) Kozhevnikov, I. V. *Catal. Rev.*−Sci. Eng. **1995**, *37*, 311. (g) Neumann, R. *Prog. Inorg. Chem.* **1998**, *47*, 317. (h) Okuhara, T.; Mizuno, N.; Misono, M. *Adv. Catal.* **1996**, *41*, 113. (i) Kuznetsova, L. I.; Maksimov, G. M.; Likholobov, V. A. *Kinet. Catal.* **1999**, *40*, 622. (j) Misono, M. *Chem. Commun*. **2001**, 1141. (k) Khenkin, A. M.; Weiner, L.; Wang, Y.; Neumann, R. *J. Am. Chem. Soc.* **2001**, *123*, 8531. (l) Kozhevnikov, I. V. *Catalysts for Fine Chemicals, Vol 2. Catalysis by Polyoxometalates*; Wiley: Chichester, U.K., 2002. (m) Kozhevnikov, I. V. *Innovations Pharm. Technol.* **2003**, *3*, 96. (n) Okun, N. M.; Travis, M.; Hardcastle, K. I.; Hill, C. L. *Inorg. Chem.* **2003**, *42*, 6610. (o) Kiricsi, I. *Appl. Catal., A* **2003**, *256*, special monographic number. (p) Hill, C. L. *Angew. Chem., Int. Ed.* **2004**, *43*, 402. (q) Liu, H.; Iglesia, E. *J. Catal.* **2004**, *223*, 161. (r) Stahl, S. S. *Angew. Chem., Int. Ed.* **2004**, *43*, 3400. (s) Kholdeeva, O. A.; Vanina, M. P.; Timofeeva, N. N.; Maksimovskaya, R. I.; Trubitsina, T. A.; Melgunov, M. S.; Burgina, E. B.; Mrowiec-Bialon, J.; Jarzebski, A. B.; Hill, C. L. *J. Catal.* **2004**, *226*, 363. (t) Won, B. K.; Voitl, T.; Rodríguez-Rivera, G. J.; Dumesic, J. A. *Science*, **2004**, *305*, 1280. (u) Hetterley, R. D.; Kozhevnikova, E. F.; Kozhevnikov, I. V. *Chem. Commun.* **2006**, 782. (v) Boglio, C.; Lenoble, G.; Duhayon, C.; Hasenknopf, B.; Thouvenot, R.; Zhang, C.; Howell, R. C.; Burton-Pye, B. P.; Francesconi, L. C.; Lacote, E.; Thorimbert, S.; Malacria, M.; Afonso, C.; Tabet, J. C. *Inorg. Chem.* **2006**, *45*, 1389.

(3) (a) Gómez-García, C. J.; Coronado, E.; Ouahab, L. *Angew. Chem., Int. Ed. Engl.* **1992**, *31*, 240. (b) Coronado, E.; Gómez-García, C. J. *Comments Inorg. Chem.* **1995**, *17*, 255. (c) Clemente-Juan, J. M.; Coronado, E. *Coord. Chem. Rev.* **1999**, *361*, 193−195. (d) Ouahab, L. *Chem. Mater.* **1997**, *9*, 1909; *Coord. Chem. Rev.* **1998**, *1501*, 178−180. (e) Coronado, E.; Galán-Mascarós, J. R.; Giménez-Sáiz, C.; Gómez-García, C. J. *Adv. Mater. Opt. Electron.* **1998**, *8*, 61. (f) Kurth, D. G.; Lehmann, P.; Volmer, D.; Muller, A.; Schwahn, D. *J. Chem. Soc., Dalton Trans.* **2000**, 3989. (g) Clemente-León, M.; Coronado, E.; Delhaes, P.; Gómez-García, C. J.; Mingolaud, C. *Adv. Mater* **2001**, *13*, 574. (h) Clemente-León, M.; Coronado, E.; Gómez-García, C. J.; Martínez-Ferrero, E. *J. Cluster Sci.* **2002**, *13*, 381. (i) Clemente-Juan, J. M.; Coronado, E.; Forment-Aliaga, A.; Galán-Mascarós, J. R.; Giménez-Sáiz, C.; Gómez-García, C. J. *Inorg. Chem.* **2004**, *43*, 2689. (j) Forment-Aliaga, A.; Coronado, E.; Feliz, M.; Gaita-Ariño, A.; Llusar, R.; Romero, F. M. *Inorg. Chem.* **2004**, *43*, 8019. (k) Mialane, P.; Duboc, C.; Marrot, J.; Riviere, E.; Dolbecq, A.; Secheresse, F. *Chem.−Eur. J.* **2006**, *12*, 1950.

(4) (a) Michelon, M.; Hervé, M.; Hervé, G. *Biochim. Biophys. Acta* **1987**, *916*, 402. (b) Yamase, T.; Fujita, M.; Fukushima, K. *Inorg. Chim. Acta* **1988**, *151,* 15. (c) Chottard, G.; Hill, C. L.; Weeks, M. S.; Schinazi, R. F. *J. Med. Chem.* **1990**, *33*, 2767. (d) Inouye, Y.; Tale, Y.; Tokutake, Y.; Yoshida, T.; Yamamoto, A.; Yamase, T.; Nakamura, S. *Chem. Pharm. Bull.* **1990**, *38*, 285. (e) Barnard, D. L.; Hill, C. L.; Gage, T.; Matheson, J. E.; Huffman, J. H.; Sidwell, R.; Otto, M. I.; Schinazi, R. F. *Antiviral Res.* **1997**, *34*, 27. (f) Fukuda, N.; Yamase, T.; Tajima, Y. *Biol. Pharm. Bull.* **1999**, *22*, 463. (g) Rhule, J. T.; Hill, C. L.; Zheng, Z.; Schinazi, R. F. *Top. Biol. Inorg. Chem.* **1999**, *2,* 117. (h) Botto, I. M.; Barrio, D. A.; Egusquiza, M. G.; Cabello, C. I.; Cortizo, A. M.; Etcheverry, S. B. *Met. Ions Biol. Med.* **2002**, *7*, 159. (i) Wang, X.; Liu, J.; Li, J.; Yang, Y.; Liu, J.; Li, B.; Pope, M. T. *J. Inorg. Biochem.* **2003**, *94*, 279. (j) Wang, X.; Liu, J.; Pope, M. T. *Dalton Trans.* **2003**, 957. (k) Yamase, T. *J. Mater. Chem.* **2005**, *15,* 4773. (l) Ogata, A.; Mitsui, S.; Yanagie, H.; Kasano, H.; Hisa, T.; Yamase, T.; Eriguchi, M. *Biomed. Pharm.* **2005**, *59,* 240.

(5) Hu, C.; Wang, Y.; Li, Y.; Wang, E. *Chem J. Internet*, **2001**, *3*, http://web.chemistrymag.org/cji/2001/036022re.htm and references therein.

replace the potassium ones from the POM precursor, affording isostructural compounds with all the three dinuclear copper complexes. In contrast, there is no replacement of potassium when the sodium acetate buffer solution is used, but the final compounds are different from those obtained with the potassium buffer.

In the case of the copper(II)−phenanthroline−acetate complex, we were able to isolate two ionic hybrid compounds[7d] (rubidium or ammonium buffers) and two discrete decorated hybrid POMs,[7f] one of them of bimolecular nature (sodium acetate buffer). On the other hand, one-dimensional hybrid materials were obtained with the copper(II)−bipyridine−oxalate dimer in all buffer solutions, with the exception of the sodium one, where a discrete didecorated hybrid POM was formed.[7b,e] Here we report on the synthesis, crystal structure, and magnetic properties of two isostructural salts of a new discrete decorated hybrid POM of bimolecular nature composed of the copper(II)−oxalate−phenanthroline

(6) (a) Anderson, T. M.; Hardcastle, K. I.; Okun, N.; Hill, C. L. *Inorg. Chem.* **2001**, *40*, 6418. (b) Long, D.-L.; Kogerler, P.; Farrugia, L. J.; Cronin, L. *Dalton Trans.* **2005**, 1372.

(7) (a) Reinoso, S. Ph.D. Thesis, Universidad del País Vasco, Bilbao, Spain, 2005. (b) Reinoso, S.; Vitoria, P.; Lezama, L.; Luque, A.; Gutiérrez-Zorrilla, J. M. *Inorg. Chem.* **2003**, *42*, 3709. (c) San Felices, L.; Vitoria, P.; Gutiérrez-Zorrilla, J. M.; Reinoso, S.; Etxeberria, J.; Lezama, L. *Chem.−Eur. J.* **2004**, *10*, 5138. (d) Reinoso, S.; Vitoria, P.; San Felices, L.; Lezama, L.; Gutiérrez-Zorrilla, J. M. *Chem.−Eur. J.* **2005**, *11*, 1538. (e) Reinoso, S.; Vitoria, P.; Gutiérrez-Zorrilla, J. M.; Lezama, L.; San Felices, L.; Beitia, J. I. *Inorg. Chem.* **2005**, *44*, 9731. (f) Reinoso, S.; Vitoria, P.; San, Felices, L.; Lezama, L.; Gutiérrez-Zorrilla, J. M. *Inorg. Chem.* **2006**, *45*, 108. (g) San Felices, L.; Vitoria, P.; Gutiérrez-Zorrilla, J. M.; Lezama, L.; Reinoso, S. *Inorg. Chem.* **2006**, *45*, 7748. (h) Reinoso, S.; Vitoria, P.; San Felices, L.; Montero, A.; Lezama, L.; Gutiérrez-Zorrilla, J. M. *Inorg. Chem.* **2007**, *46*, 1237.

complex supported on copper(II)-monosubstituted Keggin clusters, E$_4$[Cu(phen)(H$_2$O)$_4$]$_2$[Cu$_4$(phen)$_4$(H$_2$O)$_4$(ox)$_3$]$_{0.6}$[Cu$_2$-(phen)$_2$(H$_2$O)$_4$(ox)]$_{0.4}$[Cu(phen)(ox)]$_{0.8}$[{SiW$_{11}$O$_{39}$Cu(H$_2$O)}$_2$-{Cu$_2$(phen)$_2$(ox)}]·20H$_2$O [E: Rb (**1**), NH$_4$ (**2**)]. These two compounds contain copper(II) ions in six different coordination environments, one belonging to the copper-monosubstituted Keggin silicotungstate and the others to five different copper−phenanthroline species that coexist in the crystal packing.

Experimental Section

Materials and Methods. The K$_8$[α-SiW$_{11}$O$_{39}$]·13H$_2$O POM precursor,[8] as well as the copper(II)−phenanthroline−oxalate complexes [Cu(phen)(H$_2$O)(ox)]·H$_2$O[9] and [Cu$_2$(phen)$_2$(NO$_3$)$_2$-(ox)],[10] was synthesized as described in the literature. All other chemicals were obtained from commercial sources and used without further purification. Carbon, hydrogen, and nitrogen were determined by organic microanalysis on a LECO CHNS 932 analyzer. Copper and rubidium were determined on a Perkin-Elmer 4110ZL analyzer. Infrared spectra (FT-IR) for solid samples were obtained as KBr pellets on a Mattson 1000 infrared spectrometer. Thermogravimetric analysis (TGA) and differential thermal analysis (DTA) were carried out on a TA Instruments SDT 2960 thermobalance under a 100 mL/min flow of synthetic air; the temperature was ramped from 20 to 800 °C at a rate of 5 °C/min. Magnetic susceptibility was measured on a Quantum Design MPMS-7 SQUID magnetometer (T range, 5−300 K; applied field, 0.1 T; diamagnetic corrections estimated from Pascal's constants). Electron paramagnetic resonance (EPR) powder spectra were recorded on a Bruker ESP300 spectrometer (X- and Q-bands) equipped with Oxford low-temperature devices (magnetic field calibration, NMR probe; determination of the frequency inside the cavity, Hewlett-Packard 5352B microwave frequency counter; maintenance of the crystal structures in the powder samples was confirmed by powder X-ray diffraction; computer simulation, WINEPR-Simfonia, version 1.5, Bruker Analytische Messtechnik GmbH).

Synthesis of Rb$_4$[Cu(phen)(H$_2$O)$_4$]$_2$[Cu$_4$(phen)$_4$(H$_2$O)$_4$(ox)$_3$]$_{0.6}$-[Cu$_2$(phen)$_2$(H$_2$O)$_4$(ox)]$_{0.4}$[Cu(phen)(ox)]$_{0.8}$[{SiW$_{11}$O$_{39}$Cu(H$_2$O)}$_2$-{Cu$_2$(phen)$_2$(ox)}]·20H$_2$O (1). Both the cationic complex [{Cu-(phen)}$_2$(ox)]$^{2+}$ (A) and the Keggin anion α-[SiW$_{11}$O$_{39}$Cu(H$_2$O)]$^{6-}$ (B) were prepared in situ: (A) To a hot aqueous solution (20 mL) of Cu(NO$_3$)$_2$·3H$_2$O (96 mg, 0.4 mmol), solutions of 1,10-phenanthroline (79 mg, 0.4 mmol) in methanol (10 mL) and oxalic acid (25 mg, 0.2 mmol) in water (10 mL) were successively added dropwise. (B) to an aqueous solution (10 mL) of CuCl$_2$·2H$_2$O (34 mg, 0.2 mmol), a solution of K$_8$[α-SiW$_{11}$O$_{39}$] (644 mg, 0.2 mmol) in a 1 M rubidium acetate/acetic acid buffer (40 mL) was added, and the reaction mixture was heated to 100 °C for 1 h. The hot solution A was added dropwise to the solution B, and a blue precipitate appeared. The reaction mixture was stirred overnight, and then, the precipitate was removed by filtration. Prismatic blue crystals suitable for X-ray diffraction were obtained from the mother liquors by slow evaporation. Anal. Calcd (found) for C$_{104}$H$_{92}$-Cu$_{10}$N$_{16}$O$_{108}$Rb$_4$Si$_2$W$_{22}$·20H$_2$O: C, 14.30 (14.22); H, 1.52 (1.47); N, 2.57 (2.48); Cu, 7.28 (7.06); Rb, 3.91 (3.79). FT-IR (cm^{-1}): oxalate, 1672 (sh), 1643 (vs); POM, 1006 (m), 948 (s), 896 (vs), 794 (vs), 741 (s), 690 (m), 540 (m), 483 (m). TGA/DTA: Thermal

analysis shows that compound **1** decomposes via three overlapping mass loss steps starting at room temperature (Figure S1 in the Supporting Information). The first one takes places below 145 °C and comprises two endothermic dehydration processes which involve the loss of both hydration and metal coordinated water molecules [calcd (found) for 34 H$_2$O: 7.01% (7.57%)]. Dehydration is followed by the release of the oxalate anions in an exothermic mass loss step below 375 °C [calcd (found) for 4 C$_2$O$_4$: 4.03% (4.29%)], after which **1** undergoes the exothermic decomposition of the phenanthroline ligands and the Keggin polyanions to lead to the final residue at 580 °C [residue calcd (found) for 10 WO$_3$ + 10 CuWO$_4$ + 2 Rb$_2$WO$_4$ + 2 SiO$_2$: 73.2% (72.6%)].

Synthesis of (NH$_4$)$_4$[Cu(phen)(H$_2$O)$_4$]$_2$[Cu$_4$(phen)$_4$(H$_2$O)$_4$-(ox)$_3$]$_{0.6}$[Cu$_2$(phen)$_2$(H$_2$O)$_4$(ox)]$_{0.4}$[Cu(phen)(ox)]$_{0.8}$[{SiW$_{11}$O$_{39}$Cu-(H$_2$O)}$_2$[Cu$_2$(phen)$_2$(ox)}]·20H$_2$O (2). The same synthetic procedure was followed using an ammonium acetate buffer, instead of the rubidium one. Prismatic blue crystals suitable for X-ray diffraction were obtained from the mother liquors by slow evaporation. Anal. Calcd (found) for C$_{104}$H$_{108}$Cu$_{10}$N$_{20}$O$_{108}$Si$_2$W$_{22}$·20H$_2$O: C, 14.76 (14.67); H, 1.76 (1.72); N, 3.31 (3.33); Cu, 7.51 (6.93). FT-IR (cm^{-1}): oxalate, 1667 (sh), 1643 (s); POM, 1003 (w), 947 (s), 897 (vs), 793 (vs), 741 (s) 690 (m), 538 (m), 486 (m). TGA/DTA: Thermal analysis shows that compound **2** decomposes via three overlapping mass loss steps starting at room temperature (Figure S1 in the Supporting Information). The first one takes places below 145 °C and comprises two endothermic dehydration processes which involve the loss of both hydration and metal coordinated water molecules [calcd (found) for 34H$_2$O: 7.24% (8.37%)]. Dehydration is followed by the release of the oxalate anions in an exothermic mass loss step below 350 °C [calcd (found) for 4C$_2$O$_4$: 4.16% (5.11%)], after which **2** undergoes exothermic decomposition of the phenanthroline ligands and the Keggin polyanions, together with the loss of the ammonium cations, to lead to the final residue at 610 °C [residue calcd (found) for 12 WO$_3$ + 10 CuWO$_4$ + 2SiO$_2$: 71.1% (69.8%)].

X-ray Data Collection and Structure Determination. Experimental details and crystal data for compounds **1** and **2** are given in Table 1. Data collection for the single-crystal X-ray studies of both compounds was performed at room temperature on a Xcalibur diffractometer (graphite-monochromated Mo Kα radiation, λ = 0.710 73 Å) fitted with a Sapphire CCD detector. A total of 1312 (1532) frames of data were collected with exposure time of 20 s (20 s) per frame, using the ω-scan technique with frame width of Δω = 0.35° (0.30°) for compound **1** (**2**). Data frames were processed (unit cell determination, intensity data integration, correction for Lorentz and polarization effects, and analytical absorption correction) using the CrysAlis software package.[11]

Neutral atom scattering factors and anomalous dispersion factors were taken from the literature.[12] The structures were solved using a combination of Patterson and direct methods (DIRDIF99)[13] and refined by full-matrix least-squares analysis with the SHELXL97 program.[14] The positions of the aromatic H atoms were calculated geometrically and refined as riding atoms using default SHELXL parameters. Copper atoms in the polyanions were disordered over

(8) Tézé, A.; Hervé, G. *J. Inorg. Nucl. Chem.* **1977**, *39*, 999.
(9) Fabretti, A. C.; Franchini, G.; Zannini, P.; Divaira, M. *Inorg. Chim. Acta* **1985**, *105,* 187.
(10) Bencini, A.; Fabretti, A. C.; Zanchini, C.; Zannini, P. *Inorg. Chem.* **1987**, *26*, 1445.

(11) Oxford Diffraction: *CrysAlis CCD and RED*, version 1.71; Oxford Diffraction Ltd.: Oxford, U.K., 2006.
(12) *International Tables for X-ray Crystallography*; Kynoch Press: Birmingham, U.K., 1974; Vol. IV.
(13) Beurkens, P. T.; Beurkens, G.; de Gelder, R.; García-Granda, S.; Gould, R. O.; Israel, R.; Smits, J. M. M. *The DIRDIF Program System*; Crystallography Laboratory, University of Nijmegen: Nijmegen, The Netherlands, 1999.
(14) Sheldrick, G. M. *SHELXL97*; University of Göttingen: Göttingen, Germany, 1999.

Table 1. X-ray Crystallographic Data for Compounds **1** and **2**

param	1	2
molecular formula	$C_{104}H_{132}Cu_{10}N_{16}O_{128}$-$Rb_4Si_2W_{22}$	$C_{104}H_{148}Cu_{10}N_{20}O_{128}$-$Si_2W_{22}$
M_r	8732.4	8462.7
cryst system	triclinic	triclinic
space group	$P\bar{1}$	$P\bar{1}$
a (Å)	13.1674(2)	13.1529(3)
b (Å)	16.9263(4)	16.9438(3)
c (Å)	22.9728(6)	23.0200(5)
α (deg)	71.073(2)	71.256(2)
β (deg)	86.908(2)	86.863(2)
γ (deg)	71.451(2)	71.429(2)
V (Å^3)	4584.7(1)	4598.7(2)
Z	1	1
D_{calc} (g·cm^{-3})	3.163	3.044
μ (mm^{-1})	16.05	14.89
cryst size (mm)	$0.23 \times 0.08 \times 0.03$	$0.20 \times 0.06 \times 0.03$
θ range (deg)	2.55−27.50	2.63−27.50
collcd reflcns	34 307	34 858
indpndt reflcns (R_{int})	20 499 (0.030)	20 550 (0.034)
obsd reflcns [$I > 2\sigma(I)$]	13 659	10 181
refined params (restraints)	1084 (1)	805 (1)
goodness of fit on F^2	1.017	1.043
$R(F_o)^a$ (obsd reflcns)	0.0513	0.0420
$wR(F_o^2)^a$ (all reflcns)	0.1541	0.0933
largest diff peak/hole (e·Å^{-3})	3.53/−3.30	3.67/−2.98

^{a} $R(F_o) = \Sigma||F_o| - |F_c||/\Sigma|F_o|$; $wR(F_o^2) = \{\Sigma[w(F_o^2 - F_c^2)^2]/\Sigma[w(F_o^2)^2]\}^{1/2}$.

all tungsten positions, and their population parameters were refined without restrictions, resulting in the expected number of one copper ion/Keggin subunit. During the final refinement, only those population factors larger than 0.05 were kept and their sum was restrained to one. After we located and refined the hybrid POM, cationic complexes, rubidium cations, and water molecules in compound **1**, the residual electronic density map showed an empty planar region with many peaks at very short distances. Two of them, of high intensity, were assigned to a disordered copper atom, and a close inspection of the difference Fourier map revealed the presence of a phenanthroline and an oxalate ligand. Therefore, the residual electronic density was modeled as a rigid [Cu(phen)(ox)] fragment disordered over two positions (A and B), whose coordinates were retrieved from the [Cu(phen)(H$_2$O)(ox)]·H$_2$O compound[15] (Cambridge Structural Database[16] refcode DIVGAQ02). The final population parameters for the A and B positions were 59.3 and 40.7%, respectively. The same procedure was followed during the refinement of compound **2**, resulting in population parameters of 59.2 and 40.8% in the A and B positions, respectively. In compound **1**, thermal vibrations were treated anisotropically for all non-hydrogen atoms except those involved in disorder, whereas only W, Cu, and POM O atoms were refined anisotropically in compound **2**. All crystallographic calculations were performed using the WINGX software package.[17]

Computational Details. All the quantum calculations have been carried out using the Gaussian03 program[18] running on computers with GNU/Linux operating systems. Density functional theory and specifically Becke's hybrid method with three parameters[19] based on nonlocal exchange and correlation functionals, as implemented in Gaussian03 (B3LYP), has been used in all calculations.

Experimental data were used as the starting point in the geometry optimization of the cationic [Cu$_2$(phen)$_2$(H$_2$O)$_4$(ox)]$^{2+}$ ($S = 1$), [Cu-(phen)(H$_2$O)$_4$]$^{2+}$ ($S = 1/2$), and neutral [Cu(phen)(H$_2$O)(ox)] (C_s,

$S = 1/2$) complexes. The standard 6-31G(d)[20] basis set has been chosen for all atoms. This basis contains polarization functions[21] in all atoms, except hydrogen. Infrared and Raman spectra were calculated on the optimized geometry of the three mentioned species. The infrared active vibrational frequencies were identified using the GaussviewW 3.0 program,[22] which provides a visual representation of the vibrational modes. In all cases, the DFT-calculated infrared spectra were in good agreement with the experimental ones, so that a complete band assignment of the latter could be given by comparison with the former.

Results and Discussion

Synthesis and Characterization. In contrast to the big majority of TM-complex-containing POM hybrids, which are synthesized by hydrothermal techniques,[23] compounds **1** and **2** were obtained under open-air mild reaction conditions by a self-assembly process of the in situ generated [{Cu(phen)}$_2$-(ox)]$^{2+}$ and [SiW$_{11}$O$_{39}$Cu(H$_2$O)]$^{6-}$ building blocks. As can be seen in Scheme 2, the type of buffer employed as reaction media has a decisive influence in both the composition and dimensionality of the final compounds. Thus, when sodium buffer is employed, the oxalate bridging ligand in the metalorganic building block is replaced by two acetate anions, giving rise to the potassium salt of the hybrid polyanion [{Si$_2$W$_{22}$Cu$_2$O$_{78}$(H$_2$O)}{Cu$_2$(phen)$_2$(H$_2$O)(ac)$_2$}]$^{8-}$, previously reported by our group.[7f] On the other hand, using the potassium acetate medium, single crystals of the neutral monomeric complex [Cu(H$_2$O)(ox)(phen)]·H$_2$O,[9] together

(18) Frisch, M. J.; Trucks, G. W.; Schlegel, H. B.; Scuseria, G. E.; Robb, M. A.; Cheeseman, J. R.; Montgomery, J. A., Jr.; Vreven, T.; Kudin, K. N.; Burant, J. C.; Millam, J. M.; Iyengar, S. S.; Tomasi, J.; Barone, V.; Mennucci, B.; Cossi, M.; Scalmani, G.; Rega, N.; Petersson, G. A.; Nakatsuji, H.; Hada, M.; Ehara, M.; Toyota, K.; Fukuda, R.; Hasegawa, J.; Ishida, M.; Nakajima, T.; Honda, Y.; Kitao, O.; Nakai, H.; Klene, M.; Li, X.; Knox, J. E.; Hratchian, H. P.; Cross, J. B.; Bakken, V.; Adamo, C.; Jaramillo, J.; Gomperts, R.; Stratmann, R. E.; Yazyev, O.; Austin, A. J.; Cammi, R.; Pomelli, C.; Ochterski, J. W.; Ayala, P. Y.; Morokuma, K.; Voth, G. A.; Salvador, P.; Dannenberg, J. J.; Zakrzewski, V. G.; Dapprich, S.; Daniels, A. D.; Strain, M. C.; Farkas, O.; Malick, D. K.; Rabuck, A. D.; Raghavachari, K.; Foresman, J. B.; Ortiz, J. V.; Cui, Q.; Baboul, A. G.; Clifford, S.; Cioslowski, J.; Stefanov, B. B.; Liu, G.; Liashenko, A.; Piskorz, P.; Komaromi, I.; Martin, R. L.; Fox, D. J.; Keith, T.; Al-Laham, M. A.; Peng, C. Y.; Nanayakkara, A.; Challacombe, M.; Gill, P. M. W.; Johnson, B.; Chen, W.; Wong, M. W.; Gonzalez, C.; Pople, J. A. *Gaussian 03*, revision C.02; Gaussian, Inc.: Wallingford, CT, 2004.

(19) Becke, A. D. *J. Chem. Phys.* **1993**, *98*, 5648.

(20) (a) Wachters, A. J. H. *J. Chem. Phys.* **1970**, *52*, 1033. (b) Hay, P. J. *J. Chem. Phys.* **1977**, *66*, 4377. (c) Raghavachari, K.; Trucks, G. W. *J. Chem. Phys.* **1989**, *91*, 1062.

(21) Frisch, M. J.; Pople, J. A.; Winkley, J. S. *J. Chem. Phys.* **1984**, *80*, 3265.

(22) *GaussviewW*, version 3.0; Gaussian, Inc.: Wallingford, CT, 2004.

(23) For some recent examples, see: (a) Hagrman, P. J.; Zubieta, J. *Inorg. Chem.* **2000**, *39*, 5218. (b) Xu, Y.; Zhang, K.-L.; Zhang, Y.; You, X.-Z.; Xu, J.-Q. *Chem. Commun.* **2000**, 153. (c) Hagrman, P. J.; Zubieta, J. *Inorg. Chem.* **2001**, *40*, 2800. (d) Finn, R. C.; Sims, J.; O'Connor, C. J.; Zubieta, J. *J. Chem. Soc., Dalton Trans.* **2002**, 159. (e) Nandini Devi, R.;. Burkholder, E.; Zubieta, J. *Inorg. Chim. Acta* **2003**, *348*, 150. (f) Yuan, M.; Li, Y.; Wang, E.; Tian, C.; Wang, L.; Hu, C.; Hu, N.; Jia, H. *Inorg. Chem.* **2003**, *42*, 3670. (g) Luan, G.; Li, Y.; Wang, S.; Wang, E.; Han, Z.; Hu, C.; Hu, N.; Jia, H. *Dalton Trans.* **2003**, 233. (h) Lisnard, L.; Dolbecq, A.; Mialane, P.; Marrot, J.; Sécheresse, F. *Inorg. Chim. Acta* **2004**, *357*, 845. (i) Lisnard, L.; Dolbecq, A.; Mialane, P.; Marrot, J.; Codjovi, E.; Sécheresse, F. *Dalton Trans.* **2005**, 3913. (j) Gu, X.; Peng, J.; Shi, Z.; Chen, Y.; Han, Z.; Wang, E.; Ma, J.; Hu, N. *Inorg. Chim. Acta* **2005**, *358*, 3701. (k) Soumahoro, T.; Burkholder, E.; Ouellette, W.; Zubieta, J. *Inorg. Chim. Acta* **2005**, *358*, 606.

(15) Chen, X.-F.; Cheng, P.; Liu, X.; Zhao, B.; Liao, D.-Z.; Yan, S.-P.; Jiang, Z.-H. *Inorg.Chem.* **2001**, *40*, 2652.

(16) Allen, F. H. *Acta Crystallogr.* **2002**, *B58*, 380.

(17) Farrugia, L. J. *J. Appl. Crystallogr.* **1999**, *32*, 837.

Scheme 2
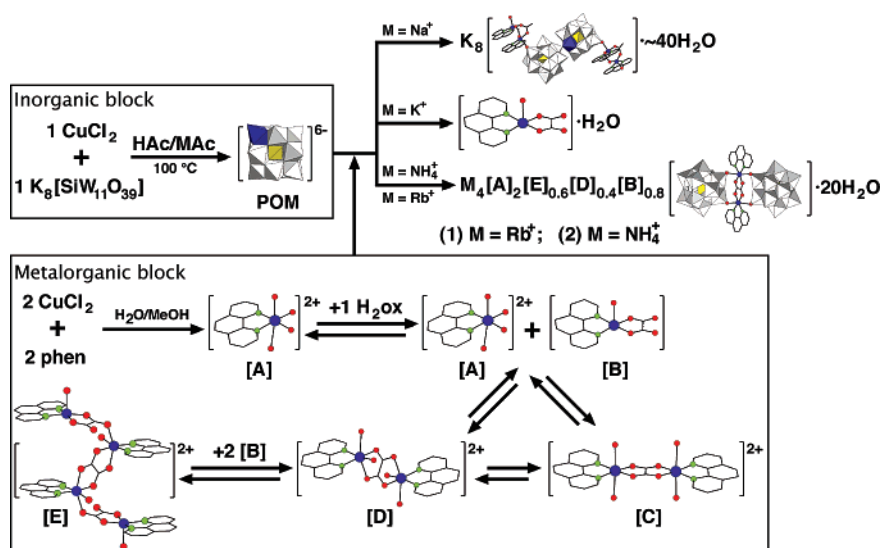
with a small amount of powder of an unidentified POM salt, are obtained. Finally, in the case of the ammonium and rubidium acetate buffers the two isostructural compounds $E_4[Cu(phen)(H_2O)_4]_2[Cu_4(phen)_4(H_2O)_4(ox)_3]_{0.6}[Cu_2(phen)_2-(H_2O)_4(ox)]_{0.4}[\{SiW_{11}O_{39}Cu(H_2O)\}_2\{Cu_2(phen)_2(ox)\}][Cu-(phen)(ox)]_{0.8}\cdot20H_2O$ [E: Rb (**1**) and NH_4 (**2**)] are isolated.

The infrared spectrum of the monosubstituted Keggin POM is similar to that of the parent monolacunary species due to the fact that both polyanions show the same ideal C_s symmetry. In general, the bands of the monosubstituted cluster can be observed at wavenumbers between those corresponding to the monolacunary species and those of the complete Keggin cluster, with the exception of the $M-O_e$ antisymmetric stretching (O_e: bridging oxygen atom between edge-sharing MO_6 octahedra), which remains practically constant at ca. 795 cm^{-1} in all three polyanions. In addition, for the monosubstituted species a new band originated in the stretching of the $Cu-O$ bonds appears at around 700 cm^{-1}.[7g]

Due to the fact that several bands of the peripheral and bridging ligands are overlapped, the optimization of the copper complexes $[\{Cu(phen)(H_2O)\}_2(ox)]^{2+}$ and $[Cu(phen)-(H_2O)(ox)]$ using DFT calculations was necessary to perform an unequivocal band assignment (Table 2). The agreement between the experimental and calculated values is highly satisfactory, although the calculated bands are slightly blue-shifted, especially in the range 1800−1300 cm^{-1}, and in addition some bands corresponding to the copper complexes in the 1100−400 cm^{-1} range are disguised by those of the POM (Figure S2 in the Supporting Information). The vibrational study has allowed us to confirm the presence of oxalate ligands in both bidentate and bis(bidentate) coordination modes, since the very intense and broad band at 1643 cm^{-1} displays two shoulders at higher wavenumbers, which are due to the C=O stretching vibration of the oxalate ligand in its bidentate coordination mode.

Description of the Structures. Both compounds **1** and **2** are isostructural, and they crystallize in the triclinic space group $P\bar{1}$. Their asymmetrical units contain half a centro-

symmetric $[\{SiW_{11}O_{39}Cu(H_2O)\}_2\{Cu_2(phen)_2(\mu\text{-}ox)\}]^{10-}$ hybrid POM, one cationic $[Cu(phen)(H_2O)_4]^{2+}$ monomer, half a centrosymmetric $[Cu_4(phen)_4(H_2O)_4(\mu\text{-}ox)_3]^{2+}$ cationic tetramer (or alternatively both half a centrosymmetric $[Cu_2-(phen)_2(H_2O)_4(\mu\text{-}ox)]^{2+}$ dinuclear copper complex and a neutral $[Cu(phen)(ox)]$ monomer), two alkaline cations, rubidium (**1**) or ammonium (**2**), and 10 water molecules. The main structural feature to these two compounds is the presence in the crystal packing of five different copper−phenanthroline complexes with nuclearities ranging from 1 to 4.

The $[\{SiW_{11}O_{39}Cu(H_2O)\}_2\{Cu_2(phen)_2(\mu\text{-}ox)\}]^{10-}$ hybrid polyanion (Figure 1) can be described as the product of the condensation of one $[Cu_2(phen)_2(\mu\text{-}ox)]^{2+}$ metalorganic building block and two $\alpha\text{-}[SiW_{11}O_{39}Cu(H_2O)]^{6-}$ inorganic building blocks. The dimeric copper−oxalate complex is sandwiched by the two POMs through the apical sites, which are occupied by two POM terminal oxygen atoms belonging to the adjacent WO_6 octahedra W1 and W2. In the $\alpha\text{-}[SiW_{11}O_{39}Cu(H_2O)]^{6-}$ inorganic building block the copper atom is disordered over the whole polyanion with the exception of W1 and W2 positions, with population factors ranging from 3.2 for W5 octahedron to 15.2% for W8 in the case of compound **1** and from 3.7 to 16.9% for the same positions in compound **2**. Thus, the dicopper complex is anchored to both POMs by four Cu−O−W bridges. Table 3 displays ranges and mean values of M−O bond distances in compounds **1** and **2** compared with those of the optimized $[SiW_{11}O_{39}Cu(H_2O)]^{6-}$ and $[SiW_{12}O_{40}]^{4-}$ POMs. The centrosymmetric metalorganic building block is made of two copper atoms bridged by an oxalate anion in the usual bis-(bidentate) fashion. The copper atoms are involved in $CuN_2O_2O'O''$ chromophores in elongated octahedral 4 + 1 + 1 environment, where two oxalate O atoms and two phenanthroline N atoms form the equatorial plane. The apical positions are occupied by the terminal oxygen atoms O1 and O2 with the Cu1−O1 bond distance (2.4 Å) significantly shorter than the Cu1−O2 one (2.7 Å). In this way, the dicopper complex can be considered coordinated to the O1 atom and semicoordinated to O2.

Table 2. Wavenumber (cm^{-1}) and Assignments of Experimental and Calculated IR Spectra for [{Cu(phen)(H$_2$O)}$_2$(ox)]$^{2+}$ and [Cu(phen)(H$_2$O)(ox)] Copper Complexes and the Metalorganic Building Blocks of Compounds **1** and **2**[b]

band assgnt[a]	[{Cu(phen)(H$_2$O)$_2$}$_2$(ox)]$^{2+}$		[Cu(phen)(H$_2$O)(ox)]		**1**	**2**
	expt	calcd	expt	calcd		
ν_{as}(C=O$_t$)$_{bd}$			1707 s	1748 vs	1709 w	1711 w
			1689 vs	1735 vs	1672 sh	1667 sh
δ(H−O−H)			1656 vs	1668 m		
			1608 sh			
δ(H−O−H), ν_{as}(C=O)$_{bbd}$	1649 vs	1662 vs			1643 s	1643 s
	1610 sh	1619 m			1610 sh	1610 sh
ν_{as}(C=C) + ν_{as}(C=N)	1585 w	1598 sh	1585 m	1605 w	1586 m	1585 w
				1575 w		
ν_{as}(C=C) + ν_s(C=N)	1520 m	1535 s	1519 m	1501 w	1520 m	1518 w
ν_s(C=C) + ν_s(C=N)	1495 w	1509 sh	1491 w	1500 m	1494 sh	1491 sh
ν(ring)	1429 s	1465 m		1413 w	1428 m	1427 m
	1406 s	1442 m				
ν(ring$_c$)		1434 sh	1432 s	1433 w	1414 sh	
			1428 s	1405 w		
			1397 s			
ν_s(C=O) + ν(C=N)	1354 m	1358 s	1350 w		1343 w	1342 w
ν(ring)	1323 s	1334 sh	1320 w	1333 w	1311 w	1307 w
				1322 w		
				1301 w		
ν_s(C=O)			1287 w			
			1256 m	1279 s		
δ_{ip}(C=C−H)	1225 w	1228 w	1223 w	1206 w	1225 w	1223 w
	1153 w	1157 w	1146 w	1129 m	1148 w	1147 w
	1115 w	1115 w	1107 w	1088 m	1110 w	1109 w
breath (ring)	1039 w	1061 w	1051 w		1050 sh	1051 sh
			1034 w	1031 w		
			1000 w	1007 w		
δ_{ip}(O=C=O) + ν(Cu−O,N)$_s$			873 sh	851 w		
			864 m	845 m		
δ_{oop}(C=C−H)	849 m	855 s	853 m	832 m	857 sh	856 sh
	791 w	780 w	790 m			
δ_{ip}(O=C=O) + ν(Cu−O,N)$_{as}$	739 w	740 m	740 w	759 m		
δ_{ip}(ring) + δ_{oop}(C=C−H)	723 s	718 m	723 s	703 m	721 s	721 s
δ_{ip}(ring)	680 w	646 w	669 w	633 w	651 w	650 w
			651 w			
ν_s(Cu−O)			546 w	564 m		
δ_{oop}(O=C=O)	484 w	466 m	475 w	450 m		
breath (ring$_c$)	457 w	430 sh	431 w	421 w		
δ_{ip}(C=C=O)	434 w	417 m			433 w	432 w

^{a} Vibrational modes: ν, stretching; δ, deformation; breath, breathing; as, antisymmetric; s, symmetric; ip, in plane; oop, out of plane; bd, bidentate; bbd, bis(bidentate); O$_t$, oxalate noncoordinated oxygen in the bidentate coordination mode; ring$_c$, phenanthroline central ring. ^{b} Band intensities: w, weak; m, medium; s, strong; vs, very strong; sh, shoulder.

Two different dinuclear copper fragments with oxalate and phenanthroline as bridging and peripheral ligands, respectively, are present in the crystal structure. One of them constitutes the metalorganic block of the above-described hybrid POM, whereas the other appears either as a part of the tetrameric fragment [Cu$_4$(phen)$_4$(H$_2$O)$_4$(ox)$_3$]$^{2+}$ (form A) or as an isolated dimeric cationic species [Cu$_2$(phen)$_2$(H$_2$O)$_2$-(ox)]$^{2+}$ (form B) depending on the disorder of the associated monomeric neutral moiety [Cu(ox)(phen)] (Figure 2). Both dinuclear fragments present a different geometry between them and with respect to the C_{2h}-symmetry optimized [Cu$_2$-(phen)$_2$(H$_2$O)$_4$(ox)]$^{2+}$ fragment, which has a chair conformation very similar to that of the nitrate derivative [Cu$_2$(phen)$_2$-(NO$_3$)$_2$(ox)].[10] Thus, in the metalorganic block of the hybrid POM the oxalato ligand adopts a bis(bidentate) symmetric coordination fashion with the oxygen atoms located in the equatorial plane and the phenanthroline ligands coplanar, the torsion angle with the oxalate plane being close to 10°. In contrast, in the nonsupported dimeric fragment [Cu$_2$(phen)$_2$-(H$_2$O)$_2$(ox)]$^{2+}$, 60% as tetrameric cationic complex (form A) and 40% as isolated dinuclear complex (form B), the oxalate

ligand presents an asymmetric bis(bidentate) coordination mode and coordinates to each copper center through one equatorial (ca. 1.95 Å) and one axial (ca. 2.20 Å) site, in such a way that it lays on a plane perpendicular to the equatorial planes of the metallic centers, with an angle between these planes and the Cu2−Cu2′ axis close to 43°. The equatorial positions are completed by two phenanthroline N atoms and one water molecule, while the remaining axial site is occupied in the form A by an oxalate O atom of the neutral fragment [Cu(ox)(phen)], leading to the [Cu$_4$(phen)$_4$(H$_2$O)$_4$-(ox)$_3$]$^{2+}$ tetramer. This O atom was refined as a water molecule in the isolated dimer (form B). Besides the neutral monomeric [Cu(ox)(phen)] complex, the crystal structure also contains the monomeric cationic copper complex [Cu(phen)-(H$_2$O)]$^{2+}$, where the copper(II) center presents a 4 + 1 + 1 octahedral geometry with two phenanthroline N atoms occupying equatorial sites (Figure 3). Selected bond distances and angles for the copper(II)−phenanthroline complexes together with the DFT optimized values are shown in Table 4.

The crystal packing of the compounds can be viewed as chains along the [01$\bar{1}$] direction composed of hybrids POMs
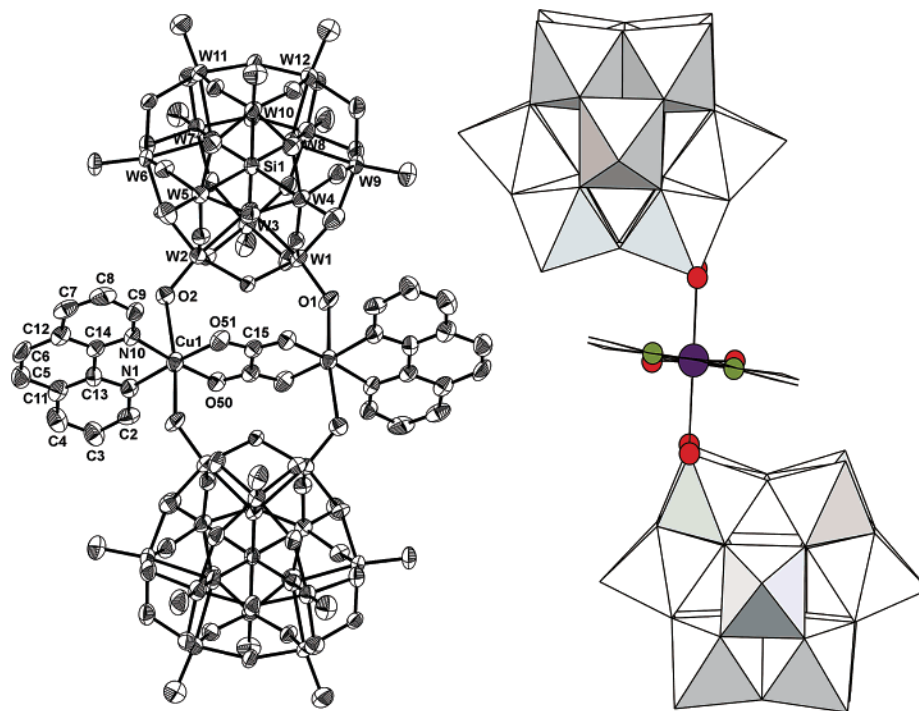
Figure 1. Left: ORTEP view of the hybrid [{SiW$_{11}$O$_{39}$Cu(H$_2$O)}$_2${Cu$_2$(phen)$_2$(μ-ox)}]$^{10-}$ polyanion in compound **1** with atom labeling. Right: Side view of a polyhedral representation of the hybrid POM.

Table 3. Range and (Mean) M−O Bond Lengths (Å) of the Inorganic Building Blocks in Compounds **1** and **2** Compared with Those of the DFT Optimized Polyanions [SiW$_{11}$O$_{39}$Cu(H$_2$O)]$^{6-}$ and [SiW$_{12}$O$_{40}$]$^{4-}$ ^{a}

			optimized polyanions		
			[SiW$_{11}$O$_{39}$Cu(H$_2$O)]$^{6-}$		
param	**1** [SiW$_{11}$O$_{39}$Cu(H$_2$O)]$^{6-}$	**2** [SiW$_{11}$O$_{39}$Cu(H$_2$O)]$^{6-}$	M = W^{VI}	M = Cu^{II}	[SiW$_{12}$O$_{40}$]$^{4-}$
M−O$_c$	2.317−2.369 (2.339)	2.315−2.361 (2.334)	2.32−2.44 (2.39)	2.319	2.325
M−O$_v$	1.868−1.945 (1.903)	1.848−1.963 (1.908)	1.81−2.03 (1.93)	2.011	1.916
M−O$_e$	1.893−1.956 (1.928)	1.881−1.991 (1.932)	1.82−2.03 (1.94)	2.018	1.937
M−O$_t$	1.702−1.748 (1.731)	1.687−1.751 (1.729)	1.76−1.77 (1.77)	2.286	1.743
Si−O$_c$	1.591−1.644 (1.623)	1.641−1.654 (1.648)	1.63−1.66 (1.65)		1.667
M···Si	3.494−3.542 (3.518)	3.499−3.550 (3.521)	3.56−3.64 (3.60)	3.377	3.588
M···M$_{trans}$	7.004−7.051 (7.031)	7.028−7.067 (7.046)	7.15−7.21 (7.19)	6.964	7.172
O···O$_{trans}$	10.41−10.46 (10.43)	10.38−10.49 (10.44)	10.61−10.69 (10.66)	10.709	10.619

^{a} Key: O$_c$, oxygen atoms belonging to the central SiO$_4$ tetrahedron; O$_v$, bridging oxygen atoms between vertex-sharing MO$_6$ octahedra; O$_e$, bridging oxygen atoms between edge-sharing MO$_6$ octahedra; O$_t$, terminal oxygen atoms.

connected through the coordination sphere of a couple of alkaline cations related by a center of inversion. These zigzagging chains are further hydrogen bonded by some water molecules to form an inorganic sublattice parallel to the *bc* plane (Figure 4). The remaining copper−phenanthroline complexes occupy the interlamellar space between adjacent inorganic layers. In this metalorganic sublattice, the [Cu$_4$(phen)$_4$(H$_2$O)$_4$(ox)$_3$]$^{2+}$ units play an important role in the stabilization of the crystal structure. As can be seen in Figure 5, the tetranuclear cations act as double clamps interconnected through π−π interactions between the phenantholine rings to form a ribbon along the [100] direction and parallel to the *ac* plane. Moreover, these phenanthrolines are involved in further π−π interactions with the phenanthroline ligands of the POM sandwiched dinuclear copper−oxalate complexes, in such a way that they connect two POM chains of adjacent layers. This packing of aromatic rings is fenced in both sides by the phenanthroline ligand of the mononuclear tetraaquacopper(II) complex, [Cu(phen)(H$_2$O)$_4$]$^{2+}$, and there-

fore eight π-interacting phenanthrolines stack along the [$\bar{1}$01] direction (Figure 6a). It must be underlined that the disorder in the [Cu(phen)(ox)] subunit of the tetranuclear complex does not substantially alter this π-stacking pattern, because the shifting, produced by rotation around the axis perpendicular to the phenanthroline plane at the C73 carbon atom, affects mainly the copper and oxalate ligand (Figure S3 in the Supporting Information). Finally, all phenanthroline aromatic rings are nearly parallel to the (11$\bar{3}$) crystallographic plane and most of them are involved in π-interactions, a fact that lends a strong stability to the metalorganic sublattice located in the *ac* plane (Figure 6b). The number of phenanthroline rings involved in these π contacts decrease when the tetranuclear copper complex is split into the dinuclear and two mononuclear copper complexes, but in contrast the number and strength of O−H···O hydrogen bonds increases.

Since it is rather unusual to find in the same crystal such variety of copper complexes bound to the same ligands, a theoretical equilibrium solution study was performed to find
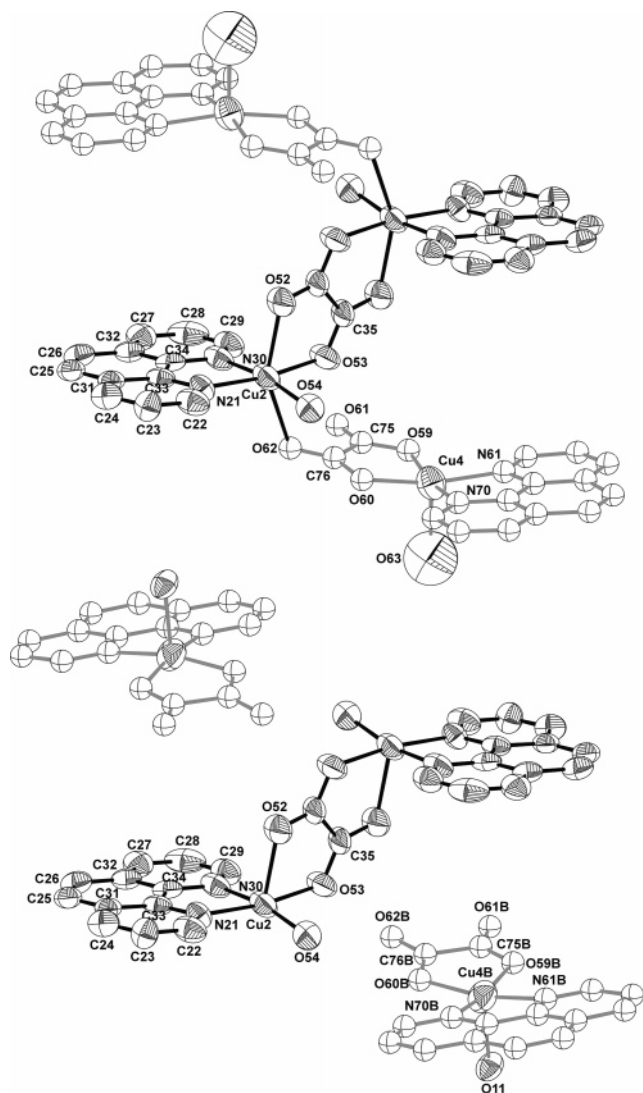
Figure 2. ORTEP views and atom labeling of the tetranuclear cationic complex $[Cu_4(phen)_4(H_2O)_4(\mu\text{-ox})_3]^{2+}$ (form A, top) and the dimeric and monomeric fragments product of tetranuclear complex splitting (form B, bottom).
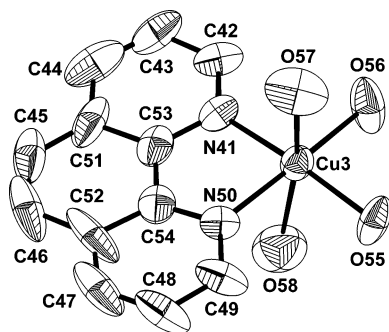
Figure 3. ORTEP view and atom labeling of the $[Cu(phen)(H_2O)_4]^{2+}$ cationic complex.

out if the species present in the solid state were predominant in aqueous solution. The simulations have been performed by means of the software MEDUSA.[24] The equilibrium constants were retrieved from the IUPAC Stability Constants

(24) Puigdomenech, I. *MEDUSA (Make Equilibrium Diagrams Using Sofisticated Algorithms)*, version 15; The Royal Institute of Technology: Stockholm, Sweden, 2001.

Table 4. Bond Lengths (Å) and Angles (deg) for the Experimental and Optimized Copper(II)−Phenanthroline Complexes in Compounds **1** and **2**[a]

	compound		
	1	**2**	optimized
{Cu$_2$(phen)$_2$(ox)}[b] in Hybrid POM			
Cu1−O50	1.96(1)	1.96(1)	1.963
Cu1−O51	1.96(1)	1.95(1)	1.965
Cu1−N1	1.99(1)	1.98(1)	1.992
Cu1−N10	1.98(1)	1.97(1)	1.995
Cu1−O1	2.42(1)	2.43(1)	2.308
Cu1−O2(i)	2.71(1)	2.73(1)	2.994
Cu1⋯Cu1(i)	5.137(2)	5.132(2)	5.112
O50−Cu1−O51	85.0(4)	85.6(3)	85.8
N1−Cu1−N10	83.2(5)	83.4(4)	83.7
O1−Cu1−O2(i)	173.0(3)	173.0(3)	162.4
W1−O1−Cu1	134.9(5)	135.9(4)	
W2−O2−Cu1(i)	128.0(5)	127.4(4)	
Cu1−phen1[c]	5.4(4)	5.0(3)	8.3
Cu1−ox1	4.8(4)	4.6(3)	18.3
phen1−ox1	10.2(4)	9.5(3)	26.6
equatorial distortion Cu1[d]	9.6(4)	9.1(3)	1.4
{Cu$_2$(phen)$_2$(ox)} in Di- and Tetranuclear Cations			
Cu2−O53	1.97(1)	1.93(1)	
Cu2−O54	2.00(1)	2.03(1)	
Cu2−N21	2.01(1)	2.02(1)	
Cu2−N30	2.02(1)	1.95(1)	
Cu2−O52	2.22(1)	2.24(1)	
Cu2−O62(iii)	2.58(1)	2.55(1)	
Cu2⋯Cu2(ii)	5.459(3)	5.463(2)	
O53−Cu2−N21	171.3(5)	171.8(5)	
O53−Cu2−O52	79.7(5)	79.0(4)	
O54−Cu2−N30	169.8(5)	167.9(4)	
N21−Cu2−N30	81.8(5)	81.4(5)	
Cu2−phen2	6.9(4)	8.1(3)	
Cu2−ox2	86.2(6)	89.8(5)	
phen2−ox2	81.0(5)	80.6(5)	
equatorial distortion Cu2	11.2(5)	13.9(3)	
[Cu(phen)(H$_2$O)$_4$]$^{2+}$			
Cu3−O55	1.98(1)	1.98(1)	2.020
Cu3−O56	1.98(1)	1.94(1)	2.055
Cu3−N41	1.99(1)	1.98(2)	1.980
Cu3−N50	1.98(1)	1.96(1)	1.980
Cu3−O57	2.30(1)	2.30(1)	2.384
Cu3−O58(iii)	2.80(2)	2.83(1)	2.625
N41−Cu3−N50	83.1(5)	82.8(5)	84.7
O55−Cu3−N41	173.8(5)	174.9(4)	180.0
O56−Cu3−N50	171.6(5)	172.6(4)	161.2
O57−Cu3−O58(iii)	173.0(5)	173.0(4)	152.2

[a] Symmetry codes: (i) $2 - x$, $1 - y$, $2 - z$; (ii) $1 - x$, $3 - y$, $1 - z$; (iii) $1 - x$, $2 - y$, $1 - z$. [b] Optimization of the $[Cu_2(phen)_2(H_2O)_4(ox)]^{2+}$ dimer in both POM supported complex and tetranuclear cation converges to the same geometry. [c] Planes: Cu1, O50, O51, N1, N10; ox1, O50, O51, C15, O50(i), O51(i), C15(i); phen1, N1, N10, C2−C14; Cu2, O53, O54, N21, N30; ox2, O52, O53, C35, O52(ii), O53(ii), C35(ii); phen2, N21, N30, C22−C34. [d] Equatorial distortions defined by the torsion angles N1−N10−O51−O50 (Cu1) and N21−N30−O53−O54 (Cu2).

DataBase,[25] except the formation constants of the Cu:ox: phen ternary system, which are not available in the literature. They were replaced by those of the Cu:ox:bpy system,[26] due to the similarity of the constants of the binary copper:phen and copper:bpy complexes.[27] As can be seen in the speciation curves (Figure 7), the only species present in significant amount below pH = 6 are the ones involved in the formation of the crystal packing of compounds **1** and **2**: the mono-

(25) *IUPAC Stability Constant Database (SC-Database),* version 4.06; Academic Software: Otley, U.K., 1999.
(26) Castro, I.; Faus, J.; Julve, M.; Muñoz, M. C.; Díaz, W.; Solans, X. *Inorg. Chim. Acta* **1991**, *179*, 59.
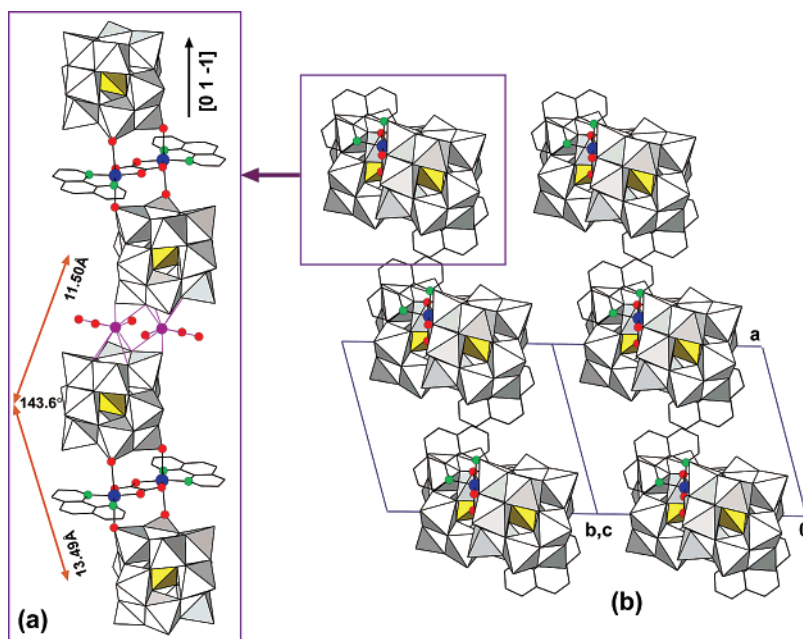
Figure 4. (a) Selected Si⋯Si distances and zigzagging angle in the chains of the hybrid POMs along the [01$\bar{1}$] direction. (b) View along the [01$\bar{1}$] direction of adjacent inorganic layers placed in the *bc* plane.
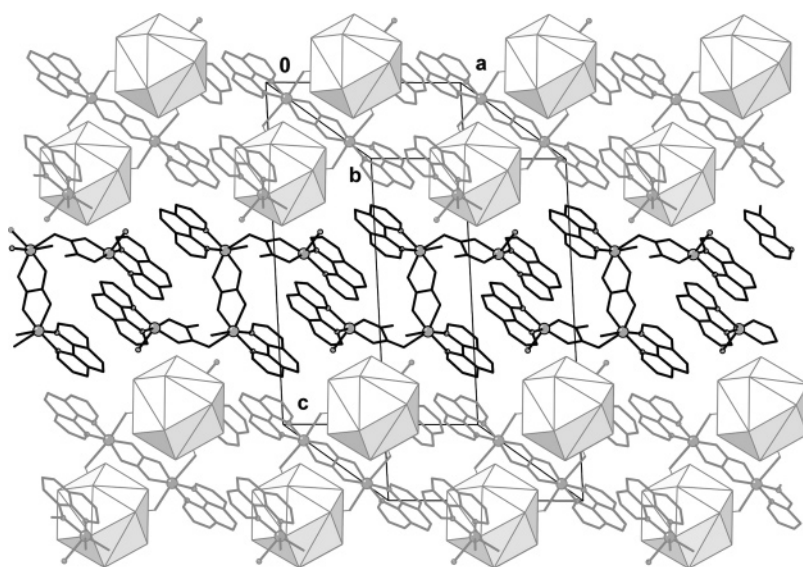
Figure 5. View in the *ac* plane of the metalorganic sublattice formed by the embrace of tetranuclear copper complexes (double clamps) through the π-interactions. The Keggin POMs are represented as cuboctahedra for clarity.

and dinuclear copper:oxalate:phenanthroline complexes [Cu-(phen)(ox)] and [Cu$_2$(phen)$_2$(ox)]$^{2+}$ and the cationic copper complex [Cu(phen)]$^{2+}$.

EPR Spectroscopy. Figure 8 shows the low-temperature X- and Q-band EPR powder spectra for compound **1**, together with their best fit (similar results obtained for compound **2** are included in the Supporting Information as Figure S4). The room-temperature X-band spectra of compounds **1** and **2** display a single anisotropic broad resonance centered at ca. 3250 G. When Q-band experiments are performed, the resolution of the spectra is considerably

improved and a signal with apparent axial symmetry is observed between 10 200 and 12 200 G. In addition, a broad shoulder of weak intensity can be detected at ca. 10 100 G. According to previous studies in analogous systems,[7a] this shoulder can be assigned to the parallel component of the axial signal generated by the Cu^{II}-monosubstituted Keggin subunits.

The spectra do not undergo significant changes as the temperature is lowered. This fact, together with the absence of hyperfine structures or half-field signals, indicates that a non-negligible magnetic interaction has to be established between all the copper(II) chromophores present in the crystal structures of compounds **1** and **2**, with the exception of the POM−Cu^{II} ion, which remains magnetically isolated. Therefore, the observed spectra correspond to an exchange **g** tensor

(27) (a) McBryde, W. A. E. *A Critical Review of Equilibrium Data for Proton and Metal Complexes of 1,10-Phenanthroline, 2,2′-Bipyridyl, and Related Compounds (IUPAC Chemical Data Series No. 17)*; Pergamon Press: Oxford, U.K., 1978. (b) Tanaka, M. *Bull. Chem. Soc. Jpn.* **2005**, *78*, 1644.
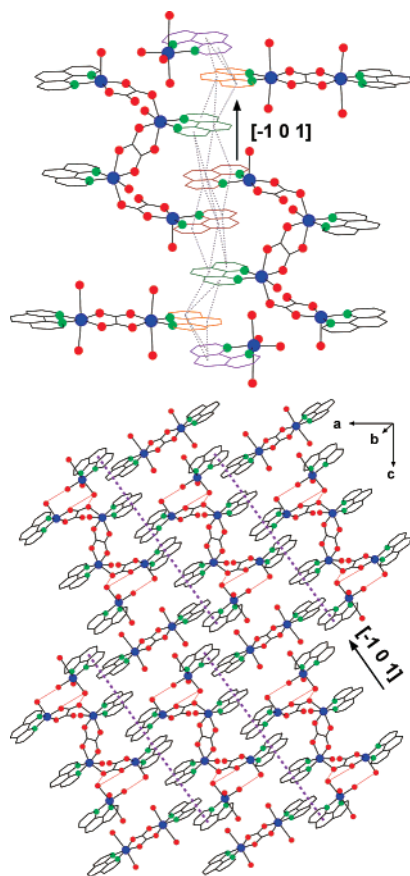
Figure 6. (Top) Detail of π-interactions between the aromatic rings of the phenanthroline ligands belonging to the following copper complexes: Cu3−Cu1−Cu2−Cu4−Cu4−Cu2−Cu1−Cu3. (Bottom) Metalorganic sublattice located in the *ac* plane with all aromatic rings nearly parallel to the (11$\bar{3}$) crystallographic plane.
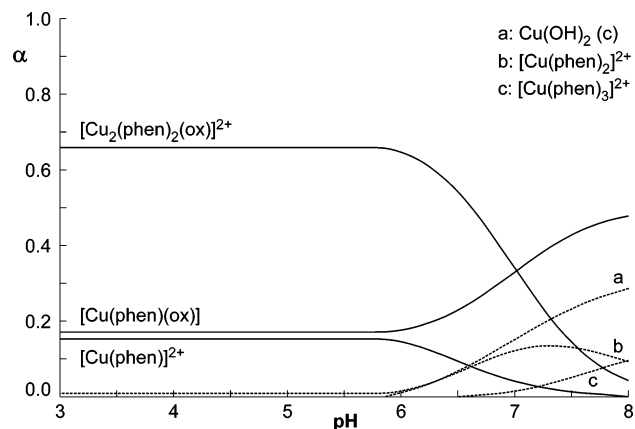

Figure 7. Distribution diagram α vs pH for aqueous solutions of copper-(II), phenanthroline, and oxalic acid. Molar fractions are referred to total Cu(II) ($C_{Cu} = C_{Phen} = 0.10$, $C_{ox} = 0.050$ mol·dm^{-3}).

and they do not reflect the individual characteristics of any Cu(II) cromophore. In compound **1**, the values obtained for the principal components of the **g** tensor from the low-temperature X- and Q-band spectra were $g_1 = 2.285$, $g_2 = 2.109$, $g_3 = 2.071$ ($<g> = 2.155$) and $g_1 = 2.285$, $g_2 = 2.096$, $g_3 = 2.065$ ($<g> = 2.149$), respectively. In compound **2**, the obtained values were $g_1 = 2.285$, $g_2 = 2.112$, $g_3 = 2.068$ ($<g> = 2.155$) and $g_1 = 2.285$, $g_2 = 2.098$, $g_3 = 2.066$ ($<g> = 2.150$), respectively.
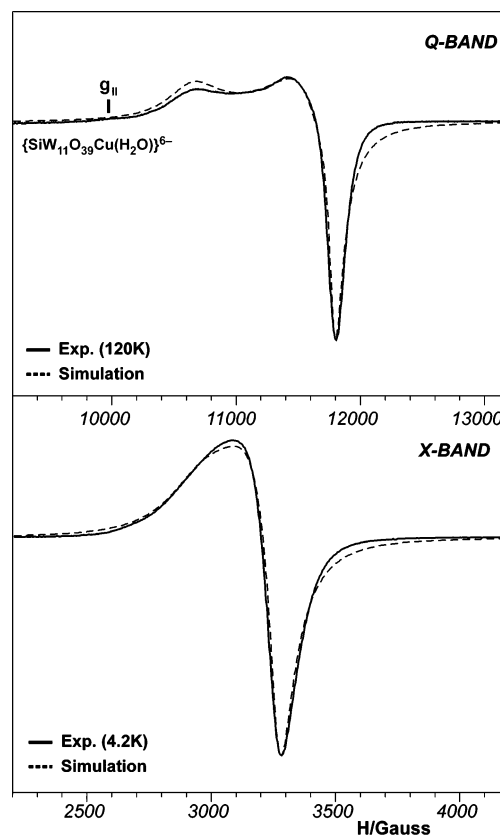
Figure 8. EPR powder spectra for compound **1**. Top: Low-temperature Q-band spectrum (120 K). Bottom: Low-temperature X-band spectrum (4.2 K). Dashed lines represent the best fit to a rhombic signal.
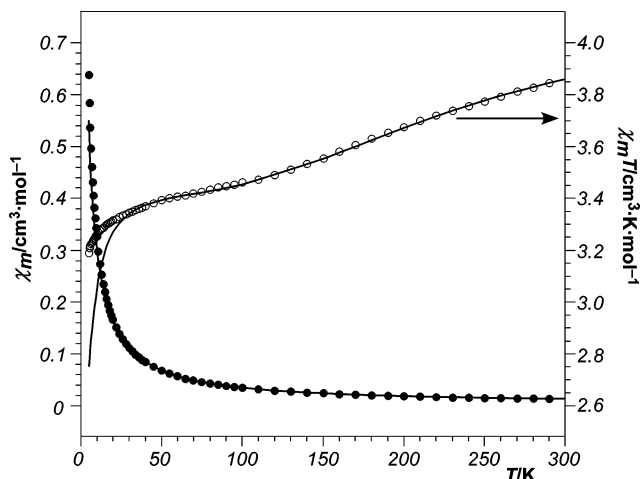
Figure 9. Thermal evolution of the magnetic susceptibility and $\chi_m T$ product for compound **1**. Continuous lines correspond to the best least-squares fit to eq 1.

Magnetic Properties. The thermal evolution of the magnetic molar susceptibility and the $\chi_m T$ product ($\chi_m T = \mu_{eff}^2/8$) is displayed in Figure 9 for compound **1** and in the Supporting Information for compound **2** (Figure S5). In both cases, the χ_m curve increases continuously with decreasing temperature and neither a maximum nor a Curie−Weiss behavior is observed even at the high temperatures. The room temperature $\chi_m T$ values are 3.864 and 3.857 cm^3·K·mol^{-1} for compounds **1** and **2**, respectively, which are in good agreement with that expected for 10 noncorrelated Cu^{II} ions (3.750 cm^3·K·mol^{-1}, considering $g = 2$). When the systems

are cooled, the $\chi_m T$ product undergoes two consecutive and partially overlapped decreasing steps. The first one is rapid and takes places between 300 and ca. 80 K, whereas the second one (from ca. 80 to 5 K) is much slower and finishes at 5 K with $\chi_m T$ values of 3.190 and 3.145 cm^3·K·mol^{-1} for compounds **1** and **2**, respectively.

This behavior indicates the simultaneous presence of two independent magnetic interactions, a very strong and a relatively weak antiferromagnetic coupling, which determine the $\chi_m T$ curve shape above and below 80 K, respectively. This observation is concordant with the fact that compounds **1** and **2** contain two different (μ-oxalato)dicopper(II) complexes, the [Cu$_2$(phen)$_2$(ox)]$^{2+}$ metalorganic block (MB) and the [Cu$_2$(phen)$_2$(H$_2$O)$_2$(ox)]$^{2+}$ dinuclear cationic fragment (DCF). The former shows a planar conformation in which the Cu^{II}-equatorial planes are almost coplanar with the oxalate anion (coplanar orbital topology), whereas in the ladderlike conformation of the latter the equatorial planes are parallel to each other and almost perpendicular to the bridging ligand (parallel orbital topology).

It is well-known that, in (μ-oxalato)dicopper(II) complexes with a coplanar orbital topology, the Cu^{II}-equatorial d$_{x^2-y^2}$ magnetic orbital is directed toward the oxalate frontier orbitals; the antiferromagnetic contribution is therefore maximized, and J values ranging from -300 to -400 cm^{-1} are usually observed. In contrast, the overlap between the Cu^{II}-magnetic and the ox-frontier orbitals is practically nonexistent when the complex exhibits a parallel orbital topology. This fact minimizes the antiferromagnetic contribution until being comparable to the ferromagnetic one, and therefore, weak coupling constants close to zero are obtained, either of ferro- or antiferromagnetic nature.[28] These antiferromagnetic interactions involve the Cu^{II} ions forming part of the copper-oxalate dimers, whereas the remaining Cu^{II} ions show a paramagnetic contribution, which masks any expected local maximum in the χ_m curve.

An exact theoretical treatment of the experimental data for compounds **1** and **2** is extremely complicated due to the simultaneous presence in the crystal structures of the two different types of (μ-oxalato)dicopper(II) complexes and three additional Cu^{II} monomeric species, the [SiW$_{11}$O$_{39}$Cu(H$_2$O)]$^{6-}$ Keggin subunit (POM), the [Cu(phen)(H$_2$O)$_4$]$^{2+}$ cation (MC), and the {Cu(phen)(ox)} neutral fragment (MNF). The absence of significant peaks in the susceptibility curves and the disorder of the MNF complex over two crystallographic positions, which gives rise to the formation of the tetrameric cation [Cu$_4$(phen)$_4$(H$_2$O)$_4$(ox)$_3$]$^{2+}$ upon coordination to the DCF complex, constitute additional factors that make difficult the fitting of the experimental data. To obtain an operative expression for the magnetic susceptibility that allows us to evaluate the strength of the different exchange interactions, some approximations are needed to reduce the large number of adjustable parameters. First, all intermolecular magnetic interactions have been intentionally discarded, in such a way that the magnetic behavior of compounds **1** and **2** has been considered as the sum of the independent contributions of two antiferromagnetic dimers and six paramagnetic monomers per formula unit. Thus, the experimental curves have been compared with those calculated with the following general expression:

$$\chi_m = \frac{2Ng^2\beta^2}{kT[3 + \exp(-J_{MB}/kT)]} + \frac{2Ng^2\beta^2}{kT[3 + \exp(-J_{DCF}/kT)]} + 6\frac{2Ng'^2\beta^2}{4kT} \quad (1)$$

Here N, β, and k have their usual meaning, g is the average g-factor of the copper-oxalate dimers, and g' is the average g-factor of the Cu^{II} monomeric complexes. The first and second terms in the above expression are the classical Bleaney-Bowers equation for a dinuclear Cu^{II} complex,[29] where J_{MB} and J_{DCF} represent the singlet-triplet energy gaps of the MB and DCF dimers, respectively. The singlet-triplet energy gap is defined by the Hamiltonian $H = -J \cdot S_A \cdot S_B$ ($S_A = S_B = 1/2$). The last term corresponds to sum of the paramagnetic contributions of the six monomeric species. To reduce the high number of magnetic variables, the g' value was fixed to 2.160, as deduced from the EPR powder spectra. Least-squares fits of eq 1 to the data were performed by minimizing the following function:

$$R = \left\{ \sum_{i=1}^{NP} [\chi_m(\exp)_i - \chi_m(\mathrm{cal})_i]^2/(NP - NV) \right\}^{1/2} \quad (2)$$

Here NP is the number of data points and NV is the number of variable parameters. No reasonable fit could be obtained over the whole experimental curve, but if one takes only the data above 35 K, a relatively good fit could be achieved with the adjustable parameters $J_{MB} = -344$ cm^{-1}, $J_{DCF} = -11.1$ cm^{-1}, and $g = 2.11$ for compound **1** and $J_{MB} = -354$ cm^{-1}, $J_{DCF} = -11.8$ cm^{-1}, and $g = 2.12$ for compound **2**. The impossibility of fitting the experimental data below 35 K should be attributed to the formation of [Cu$_4$(fen)$_4$(H$_2$O)$_4$-(ox)$_3$]$^{2+}$ tetrameric species together with the influence of the intermolecular interactions. But if these terms are included in the analytical expression of the magnetic susceptibility, the number of adjustable parameters becomes excessively large and no realistic results can be obtained.

Even if the fit is not completely satisfactory, the calculated J values are in good agreement with the structural characteristics displayed by both (μ-oxalato)dicopper(II) complexes and they can be considered as a rather good approximation. Thus, the J_{MB} values compare well to the coupling constant observed for [{Cu(phen)(NO$_3$)}$_2$(ox)],[10,30] where the Cu^{II}-ox(phen) dimer also exhibits a coplanar orbital topology, and to the DFT-calculated singlet-triplet energy gap for the coplanar (μ-oxalato)dicopper(II) complex in [{Cu(tmen)-(H$_2$O)}$_2$(μ-ox)](ClO$_4$)$_2$·1.25H$_2$O.[28b] Moreover, the small J_{DCF} values are in principle concordant with the coupling constants

(28) (a) Julve, M.; Verdaguer, M.; Gleizes, A.; Philoche-Levisalles, M.; Kahn, O. *Inorg. Chem.* **1984**, *23*, 3808. (b) Cano, J.; Alemany, P.; Álvarez, S.; Verdaguer, M.; Ruiz, E. *Chem.—Eur. J.* **1998**, *4*, 476.

(29) Bleaney, B.; Bowers, K. D. *Proc. R. Soc. London, Ser. A* **1952**, *214*, 451.

(30) Bencini, A.; Benelli, C.; Gatteschi, D.; Zanchini, C.; Fabretti, A. C.; Franchini, G. C. *Inorg. Chim. Acta* **1984**, *86*, 169.

observed for several copper(II)−oxalate dimers with a parallel orbital topology.[28a,31]

Conclusions

Our work has shown that, in addition to copper(II)−phenanthroline−acetate and copper(II)−bipyridine−oxalate dinuclear complex cations, in situ generated copper(II)-monosubstituted Keggin silicotungstates are also reactive toward the copper(II)−phenanthroline−oxalate dimer to give the bimolecular, discrete decorated [{SiW$_{11}$O$_{39}$Cu(H$_2$O)}$_2$-{Cu$_2$(phen)$_2$(μ-ox)}]$^{10-}$ hybrid POM when the reactions are carried out under open-air mild conditions using rubidium or ammonium buffer solutions as reaction media. This hybrid POM is composed of two Keggin subunits which sandwich a planar dicopper complex with the oxalate ligand in a symmetric bis(bidentate) fashion. Interestingly, the above-mentioned copper−oxalato dimer constitutes only one of the five different copper−phenanthroline species (with nucle-arities ranging from 1 to 4) that coexist in the crystal packings of the two isostuctural compounds reported in this paper. The other four are the cationic [Cu(phen)(H$_2$O)$_4$]$^{2+}$ monomer, the neutral [Cu(phen)(ox)] monomer showing a bidentate oxalate, the cationic [Cu$_2$(phen)$_2$(H$_2$O)$_4$(μ-ox)]$^{2+}$ ladderlike dimer (with the bridging oxalate in an asymmetric bis-(bidentate) coordination fashion), and the cationic [Cu$_4$-(phen)$_4$(H$_2$O)$_4$(μ-ox)$_3$]$^{2+}$ tetramer. The tetramer is formed from the interaction of the cationic dimer and the neutral monomer when the latter occupies one of the two positions over which it is disordered. Theoretical equilibrium solution studies show that the neutral and cationic monomers and the cationic dimer are the predominant species in solution at the pH value of the reaction. DFT calculations have offered an invaluable help since they have allowed us to confirm the simultaneous presence of bidentate and bis(bidentate) oxalate anions from a complete band assignment of the experimental FT-IR spectra. The crystal packing shows inorganic layers parallel to the *bc* plane with the interlamellar space occupied by a metalorganic sublattice where a massive and intricate network of $\pi-\pi$ interactions is established between all the phenanthroline ligands, all nearly parallel to the (11$\bar{3}$) crystallographic plane, a fact that lends a strong stability to the metalorganic sublattice and forces one of the binuclear copper complexes to adopt an unusual bent configuration, less stable than the coplanar one present in the hybrid POM. EPR spectroscopy shows that all copper ions are magnetically coupled, with the exception of those belonging to the Keggin subunits, whereas magnetic susceptibility measurements indicate the simultaneous presence of two independent antiferromagnetic interactions: a strong one associated with the planar copper−oxalato dimer of coplanar orbital topology and a weak one originated from the ladderlike copper−oxalato dimer of parallel orbital topology, which predominate above and below 80 K, respectively.

Supporting Information Available: Thermogravimetric curves of compounds **1** and **2**, infrared spectra of compounds **1** and **2** and experimental and calculated infrared spectra for [{Cu(phen)(H$_2$O)}$_2$-(ox)]$^{2+}$ and [Cu(phen)(H$_2$O)(ox)], ORTEP views of the disordered {Cu(ox)(phen)} moiety in compounds **1** and **2**, EPR powder spectra for compound **2**, thermal evolution of the magnetic susceptibility and $\chi_m T$ product for compound **2**, and X-ray crystallographic files of compounds **1** and **2** in CIF format. This material is available free of charge via the Internet at http://pubs.acs.org.

IC062367W

(31) (a) Gómez-Saiz, P.; García-Tojal, J.; Maestro, M.; Mahia, J.; Lezama, L.; Rojo, T. *Eur. J. Inorg. Chem.* **2003**, 2123. (b) Tuna, F.; Pascu, G. I.; Sutter, J. P.; Andruh, M.; Golhen, S.; Guillevic, J.; Pritzkow, H. *Inorg. Chim. Acta* **2003**, *342*, 131. (c) Bag, B.; Mondal, N.; Mitra, S.; Gramlich, V.; Ribas, J.; El Fallah, M. S. *Polyhedron* **2001**, *20*, 2113. (d) Castillo, O.; Muga, I.; Luque, A.; Gutiérrez-Zorrilla, J. M.; Sertucha, J.; Vitoria, P.; Román, P. *Polyhedron* **1999**, *18*, 1235. (e) Akhriff, Y.; Server-Carrió, J.; Sancho, A.; García-Lozano, J.; Escrivá, E.; Folgado, J. V.; Soto, L. *Inorg. Chem.* **1999**, *38*, 1174. (f) Smekal, Z.; Travnicek, Z.; Lloret, F.; Marek, J. *Polyhedron* **1999**, *18*, 2787. (g) Glerup, J.; Goodson, P. A.; Hodgson, D. J.; Michelsen, K. *Inorg. Chem.* **1995**, *34*, 6255.